



**BNL-102625-2013-CP**

***Use of Virtual Frisch-Grid CdZnTe Detectors to  
Attain Sub-millimeter Spatial Resolution***

**Kisung Lee**

*Presented at the 2013 IEEE NSS/MIC/RTSD*  
Seoul, Korea  
October 22 – November 2, 2013

November 2013

**Nonproliferation and National Security Department**

**Brookhaven National Laboratory**

P.O. Box 5000  
Upton, New York 11973  
[www.bnl.gov](http://www.bnl.gov)

Notice: This manuscript has been authored by employees of Brookhaven Science Associates, LLC under Contract No. DE-AC02-98CH10886 with the U.S. Department of Energy. The publisher by accepting the manuscript for publication acknowledges that the United States Government retains a non-exclusive, paid-up, irrevocable, world-wide license to publish or reproduce the published form of this manuscript, or allow others to do so, for United States Government purposes.

This preprint is intended for publication in a journal or proceedings. Since changes may be made before publication, it may not be cited or reproduced without the author's permission.

## **DISCLAIMER**

This report was prepared as an account of work sponsored by an agency of the United States Government. Neither the United States Government nor any agency thereof, nor any of their employees, nor any of their contractors, subcontractors, or their employees, makes any warranty, express or implied, or assumes any legal liability or responsibility for the accuracy, completeness, or any third party's use or the results of such use of any information, apparatus, product, or process disclosed, or represents that its use would not infringe privately owned rights. Reference herein to any specific commercial product, process, or service by trade name, trademark, manufacturer, or otherwise, does not necessarily constitute or imply its endorsement, recommendation, or favoring by the United States Government or any agency thereof or its contractors or subcontractors. The views and opinions of authors expressed herein do not necessarily state or reflect those of the United States Government or any agency thereof.

# Use of Virtual Frisch-Grid CdZnTe Detectors to Attain Sub-millimeter Spatial Resolution

Kisung Lee, *Member, IEEE*, Aleksey Bolotnikov, *Member, IEEE*, Seunghin Bae, *Student Member, IEEE*, Utpal Roy, Giuseppe Camarda, *Member, IEEE*, Matthew Petric, Yonggang Cui, *Member, IEEE*, Anwar Hossain, *Member, IEEE*, Ge Yang, *Member, IEEE*, Vaclav Dedic, *Student Member, IEEE*, Kihyun Kim, *Member, IEEE*, and Ralph James, *Fellow, IEEE*

**Abstract**—The goal of our study was twofold: To determine the distribution of signals in position-sensitive CdZnTe (CZT)-based virtual Frisch-grid detectors (VFGDs) with side-sensing pads, and to evaluate the feasibility of accurately measuring the X- and Y-coordinates where a photon interaction occurs within a single VFGD module. Accordingly, we collected signals from an anode, and from four or eight sensing pads attached to four sides of a CZT crystal. We assessed the anode's energy spectra and derived histograms from the side electrodes so to evaluate the feasibility of employing VFGDs as imaging devices. Using a highly collimated 30-keV X-ray beam at the National Synchrotron Light Source (NSLS), and applying some corrections to the raw signal data, we found that the signals acquired from one side of the detector were well separated from those measured at the opposite side. We also determined the photon interaction points by conventional Anger logic and via a more sophisticated statistics-based positioning (SBP) algorithm. With the current VFGD configuration, preliminary results showed that our positioning methods could increase the resolution above the intrinsic resolution of the VFGD (6 mm). Using SBP, we achieved a resolution below 1 millimeter for low-energy X- and gamma-rays.

## I. INTRODUCTION

Virtual Frisch-grid detectors (VFGDs) have been under development during the past few years in the Department of Nonproliferation and National Security of Brookhaven National Laboratory (BNL) for imaging and the spectroscopy of nuclear materials and gamma-ray sources [1]. Such devices offer excellent energy resolution ( $<1.5\%$  at 662 keV), along with a large effective area, consume relatively little power, and are very cost-effective. The detector employs readout electronics based on the ASIC and data-acquisition systems originally developed by BNL's Instrumentation Division for 3D devices. Currently, we are building a prototype device for imaging, which is  $6\times 6\times 15$  mm<sup>3</sup>.

However, these geometrical dimensions,  $\sim 6$  mm, limit the spatial resolution of current virtual Frisch-grid detectors. Therefore, it is critical to locate and measure the interaction points inside the crystals with our current spatial resolution, taking full advantage of the ASIC and of event-reconstruction algorithms. Information on interaction point positions within a detector area would support our more accurately correcting for charge loss, thereby enhancing the spectral performance of CZT detectors fabricated from crystals of typical quality.

The goal of this study was to accurately determine signal distributions in position-sensitive CdZnTe (CZT)-based virtual Frisch-grid detectors (VFGDs) with side-sensing pads, and to evaluate the feasibility of accurately measuring the X and Y coordinates where a photon interaction occurs within a single VFGD module.

## II. MEASUREMENT WITH UNCOLLIMATED POINT SOURCE

Fig. 1 shows the equipment that we used for these measurements, viz., the VFGD, ASIC circuit, and read-out set up. Once we had encapsulated each CZT unit with a thin polyester shell, we attached two spring-loaded contacts to the anode and cathode. Four sensing pads then were bonded to the detector's sides, as shown in Fig. 1(a). Fig. 1(b) illustrates the top view of a VFGD module. The signals collected by the four side pads indicate the strength of channels X+, X-, Y+, and Y-.

The assembled VFGD module was connected to the hardware in the test box that contains the readout electronics based on the 3D ASIC (H3D); this was developed jointly by BNL's Instrumentation Division and the University of Michigan [2]. Figs. 1 (c) and (d) show, respectively, the H3D ASIC board and the test box used for the measurement.

Initially, we employed uncollimated point sources to test the performance of the VFGD. Once the signals from the test box had been measured, the baseline of the signal was detected from its energy spectrum. Fig. 2(a) shows the spectrum we acquired from a <sup>137</sup>Cs source. This baseline is marked with a green arrow. In general, the baseline is recognized as a small peak in region of very low energy. The baseline can be changed, depending on different combinations of the ASIC's parameters, and the raw material properties of CZT. Thus, empirical, baseline detection can be conducted with the user's intervention.

---

Manuscript received November 15, 2013.

This research was supported by the U.S. Department of Energy, Office of Defense Nuclear Nonproliferation Research and Development, DNN R&D.

Kisung Lee is with the Brookhaven National Laboratory, Upton, 11973, USA, on leave from the Korea University, Seoul, Korea (telephone: +82-2940-2825, e-mail: kisung@korea.ac.kr).

Aleksey Bolotnikov, Utpal Roy, Giuseppe Camarda, Matthew Petric, Yonggang Cui, Anwar Hussein, Ge Yang, and Ralph James are with the Brookhaven National Laboratory, Upton, 11973, USA (telephone: +1-631-344-8014, e-mail: bolotnik@bnl.gov).

Seunghin Bae and Kihyun Kim are with the Radiologic Science Department, Korea University, Seoul, Korea.

Vaclav Dedic is with Charles University, Prague, Czech Republic.

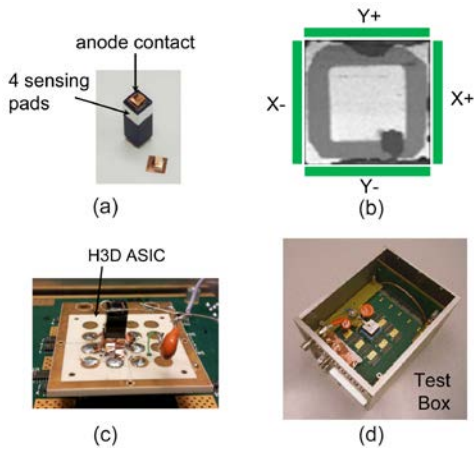


Fig. 1. The hardware of the virtual Frisch-grid detector used for measurement. (a) A VFGD module; (b) illustration of the top view of the VFGD; (c) VFGD connected to the H3D ASIC; and, (d) test box containing the VFGD, ASIC, and the read-out electronics.

Once we determined the value of the baseline, it was subtracted from the amplitude of the raw signal; Fig. 2(b) displays the results of baseline correction. The overall spectrum was shifted to the left by the amount of the detected baseline.

If the radiation source had a high-energy peak, e.g.,  $^{137}\text{Cs}$ , we also undertook a charge-loss correction (CLC). Since the tellurium inclusions in CZT detectors trap some amount of charge from the electron cloud, such defects engender random noise due to the randomly distributed interaction points. Consequently, energy peaks in the spectrum are degraded. This defect can be “corrected” first by combining position-sensing in the X-Y plane, followed by using a charge-loss-correction (CLC) technique. The results of CLC for the  $^{137}\text{Cs}$  source are displayed in Fig. 2(c). More detailed information on this correction is described in [1].

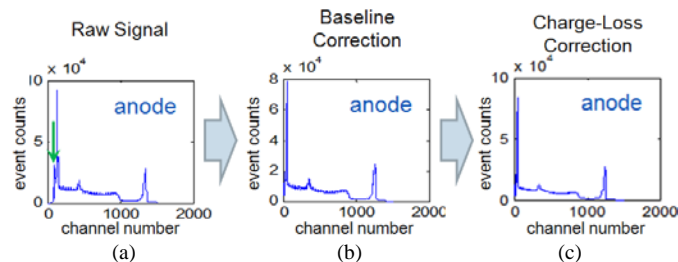


Fig. 2. Energy spectra with corrections of the measured signal from the test box. (a) Raw signal; (b) after baseline correction; and, (c) after charge-loss correction.

Fig. 3(a) shows the measured signal from four sensing pads corresponding to the anode signals displayed in Fig. 2. The green arrows point to the detected baselines of four sensing pads. After baseline- and charge-loss-corrections, the signals are changed into the spectra in Fig. 3(b).

Then, we took an energy window around the 662-keV peak and estimated the x-y positions of the incident photons that came into the VFGD. We used Anger logic [3] that employs signal proportions measured at four sensing pads for each

event. The equations that calculate the positions of x and y are as follows.

$$X = \frac{X^+ - X^-}{X^+ + X^-}, \quad Y = \frac{Y^+ - Y^-}{Y^+ + Y^-} \quad (1)$$

Fig. 4 shows the 2D position-histograms of  $^{137}\text{Cs}$  and  $^{241}\text{Am}$  sources estimated by Eq. (1). By adjusting the intensity level of the histogram, we could find the ring-shaped anode-contact at the center of the CZT crystal.

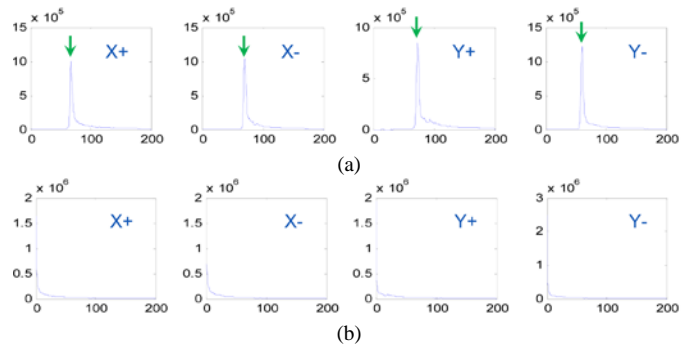


Fig. 3. Energy spectra from four sensing pads measured from a VFGD with Cs-137 point source. (a) Raw signal, and, (b) After corrections for the baseline and charge-loss. The horizontal axis of each spectrum denotes channel number, and the vertical axis represents event counts.

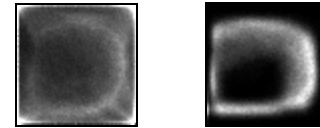


Fig. 4. Two-dimensional position histogram of Cs-137 sources (left), and Am-241(right) sources obtained by Anger logic.

We also tried to acquire an image from an Americium source that was placed on the 0.5-mm slit collimator. Fig. 5 illustrates the energy spectrum of all electrodes and their position histograms. Initially, we acquired the 2D position map before applying any corrections. The results are shown in the image labeled "raw data".

The six signal histograms in this figure show the results after baseline correction. We did not apply a charge-loss correction because we could not find any distinct benefit in doing so with a low energy source like  $^{241}\text{Am}$ . After we adopted an energy window (red rectangle in the anode spectrum in Fig. 5), and then applied Anger positioning as described in Eq. (1). Consequently, we could readily recognize the slit in the image labeled "after correction".

Knowing the positions of interaction points, we electronically segmented the area of the detectors into numerous sub-pixels (up to 3600) for which we individually applied charge-loss corrections to improve the energy resolution [4]. From these measurements, we estimated that the spatial resolution achieved was  $\sim 200 \mu\text{m}$  for X-rays above 60 keV.

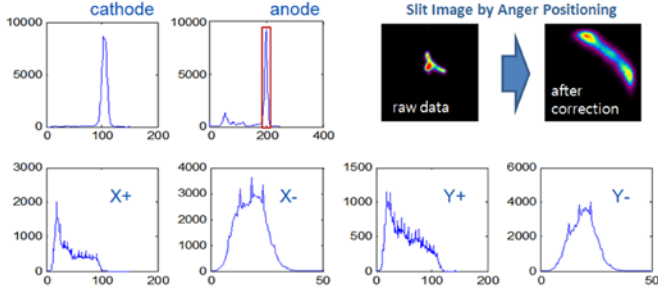


Fig. 5. Energy histograms of Am-241 source on the 0.5-mm slit after baseline correction, and 2D position maps before and after correction. The horizontal axis of each spectrum denotes channel number, and the vertical axis represents event counts.

### III. MEASUREMENT WITH HIGHLY COLLIMATED SYNCHROTRON RADIATION SOURCE

To investigate the signal properties of the sensing pads with respect to the spatial locations of incident photons, we used a collimated X-ray beam at the National Synchrotron Light Source (NSLS) [5]. The beam's size is  $10 \times 10 \mu\text{m}^2$ . We measured  $71 \times 71$  positions at  $100\text{-}\mu\text{m}$  intervals to cover the  $6 \times 6 \text{mm}^2$  detector's surface area. Fig. 6(a) illustrates the experimental setting at BNL's NSLS facility. We used eight sensing pads (two per each side) to improve our ability to separate the positions, as illustrated in Fig. 6(b). The upper image shows the layout of the eight pads attached to the side of the VFGD, while the lower image displays the  $6 \times 6$  positions of the incident photons investigated in this experiment. We marked the positions of the first column as P1 through P6. The space between two adjacent positions is 1 mm.

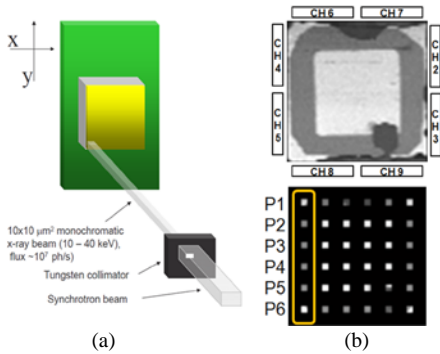


Fig. 6. Illustrations of our experiment with a highly collimated synchrotron-radiation source (a); and, layout of sensing pads and positions investigated for positioning (b). CH 1 was assigned to the anode.

We first investigated the distributions of signals with respect to the positions of incident photons. As Fig. 7 shows, a stronger signal (higher amplitude) was observed in cases where the pad was located closer to that position.

Fig. 8 shows the measured energy peaks at positions P1 through P6. We fitted the energy histogram into a Gaussian distribution, and utilized its mean to derive the plots. As

evidenced in the graphs, the signal becomes stronger as the positions are closer to the pad and vice versa.

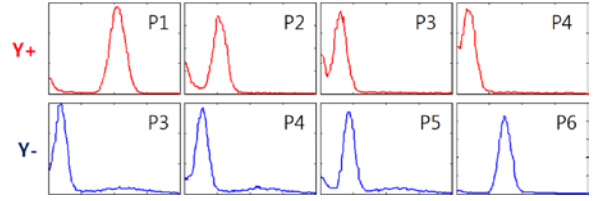


Fig. 7. Measured energy histograms of upper (Y+) and lower (Y-) sensing pads. The horizontal axis of each spectrum denotes channel number, and the vertical axis represents event counts.

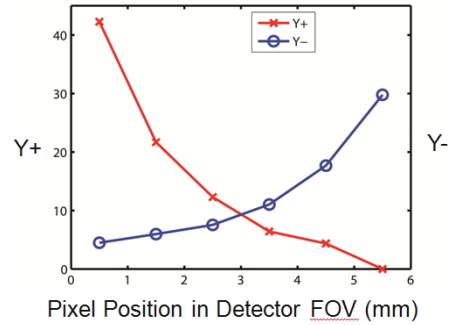


Fig. 8. Measured energy peaks at positions P1 through P6.

For proportion-based Anger positioning, we combined the signals from a pair of sensing pads at the same side to derive  $[X+, X-, Y+, Y-]$ . Each position was determined with very broad full-width-at-half-maximum values as shown in Fig. 9 (the position maps labeled P1, P3, and P5). However, when we combined all six positions (P1 through P6), we could not distinguish between them. This finding indicates that, with the conventional Anger positioning, we cannot achieve 1 mm resolution for this VFGD configuration.

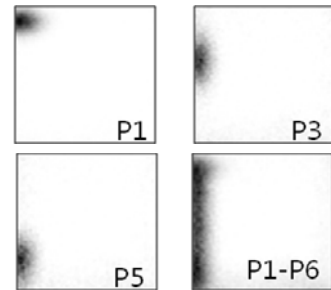


Fig. 9. Position maps generated by Anger logic for positions P1 (upper left), P3, P5, and P1 through P6 combined.

To improve the spatial separability of incident photons, we adapted a more sophisticated method based on the statistical properties of the pad signals. Eq. (2) explains the statistics-based position (SBP) method we used. We maximized the separation of signal distributions of each pad with respect to each position with multiple Gaussian mixtures ( $g_m$ ) and their weights ( $w_m$ ).

$$\tilde{S} = \underset{1 \leq k \leq K}{\operatorname{argmax}} p(\tilde{f}_e | \theta_k) = \underset{1 \leq k \leq K}{\operatorname{argmax}} \left( \log \sum_{m=1}^M w_m g_m(\tilde{f}_e) \right) \quad (2)$$

In Eq. (2),  $\tilde{S}$  is the estimated position,  $\tilde{f}_e$  is a measured channel vector for evaluation,  $K$  is the number of positions,  $w$  is the weight of the mixture  $m$ , and  $g(\cdot)$  is the Gaussian density of mixture  $m$ . Gaussian mixtures and their weights were optimized in the training step of SBP before evaluation so that their vector represents a set of parameters that can distinguish distributions as statistically unique as possible. More detailed information on this positioning algorithm is well described in [6].

In this experiment, eight sensing pads were used to maximize the signal's statistical characteristics. As shown in Fig. 10(a), the results were improved dramatically over Anger positioning. Fig. 10(b) displays the profiles through the first column of Fig. 10(a). We identified a degraded performance at P3, wherein the signal distributions of P3 are somewhat similar to those in the adjacent positions. We think some physical defects in our CZT materials, such as sub-grain boundaries or the irregular Te inclusions that degrade the detector's performance, are the cause here. However, its overall performance is promising, such that we can achieve 1 millimeter resolution even with our current experimental settings.

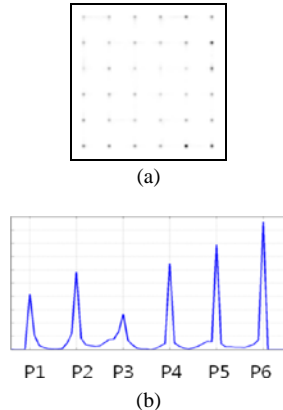


Fig. 10. Results of statistics-based positioning algorithm for 6 x 6 positions. (a) 2D position map in the inverse gray scale. (b) Profile through the first column.

#### IV. CONCLUSIONS

We investigated the feasibility of employing position-sensitive virtual Frisch-grid CdZnTe detectors with multiple sensing pads at four sides as an imaging device. We first measured the signal with point sources, and then explored it with a collimated light source (30 keV) generated at BNL's National Synchrotron Light Source facility.

Our investigation indicates that the signal collected by the pad strengthened as the position of photon interaction became closer to the pad. Our estimation of the position based on the proportions of the signals at side pads did not result in good

performance due to the noise of the signals. To improve position performance, we employed a statistics-based position-estimation algorithm; the results showed the possibility of 1-mm spatial resolution for low energy X-rays.

We will continue to better our results by refining the correction methods, improving the SBP algorithms, and undertaking more experiments with different configurations of the detector.

#### ACKNOWLEDGMENT

This research was supported by the U.S. Department of Energy, Office of Defense Nuclear Nonproliferation Research and Development, DNN R&D.

#### REFERENCES

- [1] A. E. Bolotnikov, J. Butcher, G. S. Camarda, G. De Geronimo, J. Fried, R. Gul, P. M. Fochuk, M. Hamade, A. Hossain, K. H. Kim, O. V. Kopach, M. Petryk, E. Vernon, G. Yang, and R. B. James, "Array of Virtual Frisch-Grid CZT Detectors With Common Cathode Readout for Correcting Charge Signals and Rejection of Incomplete Charge-Collection Events," *IEEE Trans. Nuc. Sci.*, vol. 59, no. 4, pp. 1544-1551, Aug. 2012.
- [2] F. Zhang, C. Herman, Z. He, G. De Geronimo, E. Vernon, and J. Fried, "Characterization of the H3D ASIC Readout System and 6.0 cm<sup>3</sup> 3-D Position Sensitive CdZnTe Detectors," *IEEE Trans. Nucl. Sci.*, vol. 59, no. 1, pp. 236-242, Feb. 2012.
- [3] Simon R. Cherry, James A. Sorenson, and Michael E. Phelps, *Physics in Nuclear Medicine*, 4th ed., Elsevier, Philadelphia, USA, 2012, pp. 199.
- [4] A. E. Bolotnikov, G. S. Camarda, G. De Geronimo, J. Fried, N. Hannah, A. Hossain, G. Mahler, K. Lee, M. Maritato, M. Marshall, M. Petryk, U. Roy, E. Vernon, G. Yang, and R. B. James, "Use of High Granularity Position Sensing to Improve the Energy Resolution of CdZnTe X- and Gamma-Ray Detectors," *Nucl. Instr. Meth. Phys. Res. A*, submitted.
- [5] Brookhaven National Laboratory National Synchrotron Light Source facility website, <http://beamlines.ps.bnl.gov/beamline.aspx?blid=X27B>.
- [6] S. Bae, K. Lee, C. Seo, J. Kim, S.-K. Joo, and J. Joung, "Novel positioning method using Gaussian mixture model for a monolithic scintillator-based detector in positron emission," *Opt. Eng.*, vol. 50, no. 9, pp. 093606, 2011.